Journal of Oil Palm Research
DOI: https://doi.org/10.21894/jopr.2022.0000

CELL WALL-GLYCOLIPIDS PROFILING OF OIL PALM ROOTS DURING *Ganoderma boninense* INFECTION USING GAS CHROMATOGRAPHY-MASS SPECTROMETRY

ALEXANDER, A[1]; ABDULLAH, S[2]; DAYOU, J[3] and CHONG, K P[4]*

ABSTRACT

Better understanding of the cell wall (CW)-glycolipids changes associated with basal stem rot (BSR) disease is essential for identifying the pathogen-host interaction to improve management and diagnostic measures. The aim of this study was to investigate the CW changes in the glycolipids profile of oil palm roots during G. boninense *infection. We carried out lipidomic analysis of glycolipids fractionated from CW-lipids of oil palm seedlings artificially infected (AI) with* G. boninense*. Oil palm roots were harvested at three (first interval) and six months (second interval) post-AI from infected and control (uninfected) seedlings and were subjected to gas chromatography-mass spectrometry (GC-MS) based global lipidomic analysis. Principal component analysis (PCA) and partial least square-discriminant analysis (PLS-DA) confirmed 11 impaired glycolipids (six in first and five in second interval) associated to cell-signalling and break down of energy. Pyruvate metabolism and glycolysis or gluconeogenesis are the most perturbed pathways during the pathogenesis as revealed by pathway impact analysis. The possible utilisation of the glycolipids as biomarkers for diagnostic of* Ganoderma *infection was authenticated using the receiver operating characteristic (ROC) curve analysis. The current research suggests five glycolipids [Phosphatidylcholine (PC)(6:0/0:0), PC(2:0/2:0), Phosphatidic Acid (PA)(18:4(6Z,(Z,12Z,15Z)/0:0), PA(14:0/ 0:0) and γ-linolenic acid] are the potential biomarkers which may be further investigated for early detection of BSR.*

Keywords: cell wall-glycolipids profile, *Ganoderma boninense*, GC-MS, oil palm root.

Received: 2 June 2020; **Accepted:** 3 December 2021; **Published online:**

[1] Agrifert Malaysia Sdn. Bhd., Unit 11.01, Level 11, Mercu 2, No. 3, Jalan Bangsar, KL Eco City, 59200 Kuala Lumpur, Malaysia.

[2] Institute for Tropical Biology and Conservation, Universiti Malaysia Sabah, Jalan UMS, 88400 Kota Kinabalu, Sabah, Malaysia.

[3] Vibration and Sound Research Group (e-VIBS), Faculty of Science and Natural Resources, Universiti Malaysia Sabah, Jalan UMS, 88400 Kota Kinabalu, Sabah, Malaysia.

[4] Biotechnology Programme, Faculty of Science and Natural Resources, Universiti Malaysia Sabah, Jalan UMS, 88400 Kota Kinabalu, Sabah, Malaysia.

* *Corresponding author e-mail: chongkp@ums.edu.my*

INTRODUCTION

Worldwide oil palm production has been steadily increased in the past years. Not only the production contributed to the majority of vegetable oils and fats, it also helps to alleviate poverty in developing countries especially in Indonesia and Malaysia. However, one of the major concerns of oil palm plantation in Southeast Asia is the basal stem rot (BSR) disease caused by *Ganoderma boninense* which could result in great loss (Tay and Chong, 2016). BSR is caused by white rot fungi, *Ganoderma* sp. The fungus grows within the palm, degrades the lignin and cellulose components of the oil palm (Mohd Aswad *et al.*, 2011).

Early detection and diagnosis of BSR disease is rather difficult with the current knowledge and technologies, due to late emergence of the BSR disease symptoms. The current detection technique was done by isolation of the fruiting bodies appearing on the oil palm trunks or primary roots near soil level followed by molecular identification of the isolated fungus (Madihah *et al*., 2018). However, it is time consuming and by the time the foliar symptoms are observed, most of the tissues will have been killed by the fungus (Ariffin *et al*., 2000). Nonetheless, the most common detection method in the field by planters is by observing the appearance of foliar symptoms or the presence of *Ganoderma* fruiting bodies. Other diagnostic tools for early detection of *G. boninense* include using *Ganoderma* Selective Medium (GSM) (Ariffin and Idris, 1992), some lab-based molecular and biochemical detection methods such as ergosterol analysis and immunoassay (Chong *et al*., 2017). Recently, many researchers attempted in developing field detection methods, these include tomography (Idris *et al*., 2009), Molecularly Imprinted Polymer (MIP) Sensors (Markon *et al*., 2008) and hyperspectral reflectral data (Lelong *et al*., 2010). Some emerging detection methods include using infrared spectroscopy (Dayou *et al*., 2014), ultrasonic (Ishaq *et al*., 2014; Najmie *et al*., 2011) and acoustics computed assisted tomography (Michael *et al*., 2020). However, most of these detection methods are still at the experimental stage, not available in the field and are not readily to serve for earlier detection purpose.

It is important to point out that early detection of BSR is crucial for better management of BSR in oil palm. An effective and robust approach is essential to achieve such objectives. The emerging lipidomics research could offer a great option in determining possible biomarkers and biochemical pathways for BSR early detection purpose. Meanwhile, plant and fungal non-cytoplasmic lipids compositions, such as those that reside in CW and cell membrane were continuously and dynamically change according to the biological, chemical and physical stresses. In oil palm-*Ganoderma* interaction, one of the promising examples is the utilisation of ergosterol. Ergosterol is the main component of the fungal membrane that is useful as biomaker for the quantification of fungal biomass (Chong *et al*., 2014; Toh Choon *et al*., 2012). The membrane lipid ergosterol is found almost exclusively in fungi and is frequently used by microbiologists as an indicator of living fungal biomass, based on the assumption that ergosterol is labile, therefore, rapidly degraded after the death of fungal hyphae (Mille-Lindblom *et al*., 2004). The main advantage with ergosterol compared to other biomarkers, such as chitin and ATP is its specific association with fungi. *G. boninense* biomass is reported to be directly correlated with ergosterol concentration; therefore, provides a reliable diagnostic method for the BSR detection (Alexander *et al*., 2017; Chong *et al*., 2012a; Mohd Aswad *et al*., 2011). However, in early stage of infection, ergosterol is difficult to be quantified due to the very small amount of fungal biomass that is present inside oil palm with addition of its labile properties. It is believed that other lipid composition, such as glycolipids are more stable than sterols, and unique due to their role in cell-cell signalling. If researchers are able to exploit the glycolipids information in plant CW and cell membrane especially during oil palm-*Ganoderma* interaction, they might be able to identify the presence of specific glycolipids compounds that are produced during early stage of infection. Therefore, the present work aimed to investigate further into glycolipids composition during oil palm-*Ganoderma* interaction. The emerging lipidomics field of research could offer a great option for determining possible biomarkers and biochemical pathways that can discriminate infected palms from those that are not infected, thus potentially providing important fundamental information for BSR early detection approach.

MATERIALS AND METHODS

Plant Material

Eight months-old oil palm commercial seedlings (*Dura* x *Pisifera*) were purchased from Sawit Kinabalu Sdn. Bhd., Beaufort, Sabah, Malaysia. The seedlings were grown in polybags (38 cm x 45 cm) with soil and sand mixture (2:1) and all seedlings were watered and fertilised using Granular NPK 15:15:6:4 following the standard agronomic practices.

Artificial Inoculation of Oil Palm Seedling using Rubber Wood Block (RWB) Technique

RWB were prepared from rubber wood. *G. boninense* UMSBRIa strain (Chong *et al*., 2013) was inoculated to the RWB as inoculum for the artificial inoculation. The method of Khairudin (1991) was adopted for preparing the RWB (size of 6 x 6 x 12 cm) with *Ganoderma* inoculum. RWB were washed with clean water, kept in autoclavable polypropylene plastic bags and autoclaved for 2 hr at 121°C. Each of the plastic bags was added with 100 ml of sterile molten malt extract agar (MEA), the agar solidified in the bags after some time. Mycelial plugs with the size of 6 mm were excised from the edge of 14 days old *G. boninense* culture and inoculated

on the RWB. The *G. boninense*-inoculated RWB were tightly sealed and kept for eight weeks in the dark and at temperature of 25 ± 2°C until fully colonised. Artificial inoculation was conducted by following Khairudin (1991). Oil palm seedlings were carefully removed from polybags and later kept seated on the *G. boninense*-inoculated RWB to ensure the roots were in direct contact with the inoculum. Twenty oil palm seedlings were inoculated with *Ganoderma* RWB while another 20 uninoculated served as healthy control. Extreme care was taken to minimise injury during inoculation and planting. All oil palm seedlings were placed and arranged in complete randomised blocks under shed house conditions with 70% of shade protection and regular watering.

Assessment of Disease Infection and Development

For the assessment of disease infection and development, method as described by Japanis *et al.* (2021) was adopted with slight modification. All the inoculated oil palm seedlings were destructively sampled to determine the colonisation and establishment of *G. boninense* at two intervals: first interval [three months after artificial inoculation (AI)] and second interval (six months after AI). Ten seedlings were destructively sampled for each of the sampling period. Roots tissues from the seedlings were harvested and washed under tap water, soaked in 99% ethanol for 30 s before being dried under ambient air stream. The infection of *G. boninense* was detected based on the isolation and *Ganoderma* growth on GSM (Ariffin and Idris, 1992) and the presence of ergosterol (Chong *et al*., 2012b). Disease incidence was calculated using the Equation (1) (Masood *et al*., 2010):

$$\text{Disease Incidence (DI)} = \frac{\text{Number of infected plants}}{\text{Total number of plants assessed}} \times 100 \quad (1)$$

Disease symptoms such as presence of fungal mass or fruiting bodies, yellowing or browning of leaf were determined using disease severity index (DSI) formula. DSI adopted from Abdullah *et al.* (2003) was used to determine the severity of the disease with score from 0 to 4 scales (*Table 1*). The DSI was calculated using the Equation (2):

$$\text{DSI} = \frac{\text{Number of seedlings in the rating} \times \text{rating number}}{\text{Total number of seedlings assessed} \times \text{highest rating}} \times 100 \quad (2)$$

To assess the internal symptoms of *Ganoderma* infection, the seedlings were cut longitudinally across the bole region. Bole damage was assessed based on the scale as described by Nursabrina *et al.* (2012) (*Table 2*).

The bole damage index was calculated based on the internal symptoms of the bole tissues using the Equation (3):

$$\text{Bole damage index} = \frac{\text{Number of seedlings in the rating} \times \text{rating number}}{\text{Total number of seedlings assessed} \times \text{highest rating}} \times 100 \quad (3)$$

TABLE 1. THE SIGNS AND SYMPTOMS OF DISEASE SEVERITY INDEX SCORED BASED ON DISEASE SCALE 0-4

Disease class	Signs and symptoms
0	Healthy plants with green leaves without appearance of fungal mycelium on any part of plants
1	Appearance of white fungal mass on any part of plants, with or without chlorotic leaves
2	Appearance of basidioma on any part of plants with chlorotic leaves (1 to 3 leaves)
3	Formation of basidioma of any part of plants with chlorotic leaves (> 3 leaves)
4	Formation of a well-developed basidioma and the plants dried

Source: Abdullah *et al*. (2003).

TABLE 2. SIGNS AND SYMPTOMS OF BOLE INDEX SCORED BASED ON 0-4

Disease class	Signs and symptoms
0	Healthy
1	up to 20% rotting of bole tissues
2	21% to 50% rotting of bole tissues
3	51% to 90% rotting of bole tissues
4	over 90% rotting of bole tissues

Source: Nursabrina *et al*. (2012).

Extraction of Cell Wall (CW)-Lipids

Oil palm root materials (100 g of fresh weight) were lyophilised for 48 hr. Then the lyophilised materials were homogenised using a commercial blender until fine powder and followed by CW isolation as described by Canut *et al.* (2016) with slight modification. CW materials were subjected to lipids extraction. Samples of *G. boninense*, healthy and infected CW (1 g) were added to 50 mL centrifuge tubes together with 10 mL of chloroform and methanol mixture with a volume ratio of 2:1. The tubes were agitated in temperature-controlled incubator shaker (Thermo Scientific Orbital and

Incubator Shaker) for 120 min at 30°C. The liquid phase was recovered with centrifugation of 1000 g for 10 min. A 0.2 volume of miliQ® water was used to wash the solvent mixtures with additional agitation for another few seconds. The two phases were further separated by centrifugation at 1000 g. The lower chloroform phase which contained the lipids was kept for further use while the aqueous upper phase was removed. A stream of N_2 at temperature of 25 ± 2°C was used to dry the extracts.

Fractionation of CW-Lipids Using Solid Phase Extraction (SPE)

Fractionation of CW lipids extracts were performed using a Strata SI-1 silica disposable cartridge column (500 mg/6 mL) (Phenomenex) as described by Stobiecki *et al*. (1997) with slight modifications. The cartridge column was equilibrated by rinsing twice with 2 mL of chloroform using SPE manifold. Crude CW lipids dissolved in 2 mL of chloroform were loaded onto the column and the solvent was pulled through. Thereafter, the column was eluted with 10 mL of chloroform to elute sterol and neutral lipids fractions. Then, 10 mL of acetone and methanol mixture (9:1) was applied to elute glycolipid fraction. Finally, free fatty acids and phospholipid were eluted using 10 mL of methanol. Each fraction collected was dried under stream of nitrogen (N_2) prior to high-performance thin layer chromatography (HPTLC) analysis.

Permethylation of Glycolipids

Glycolipids permethylation was performed as described by Longo *et al.* (2013). Under N_2 stream, glycolipids were dried and stored overnight at 20°C with silica gel. The glycolipids were later suspended in 150 µL of anhydrous dimethyl sulphoxide (DMSO), agitated with few milligrams of anhydrous sodium hydroxide (NaOH) and 80 µL of iodomethane before incubated and shaken for 1 hr at temperature of 25 ± 2°C. Dichloromethane (2 mL) and deionised water (2 mL) were added to the mixture, agitated and centrifuged for removal of the aqueous upper layer. Two mL of deionised water was used to wash the organic phase for three times before dried under N_2 stream.

Gas Chromatography-Mass Spectrometry (GC-MS) Analysis of Glycolipids

The GC-MS analysis of glycolipids was performed using GC-MS (Agilent, 5975C) with J&W GC column (30 m x 250 µm × 0.25 µm; Agilent) according to method described by Nyberg (1986) with some modifications. For GC-MS detection, an electron ionisation system with ionisation energy of 70 eV was used. The injector temperature was maintained at 280°C. The carrier gas (helium) was set at the flow rate of 1.0 mL/min before the sample (1.0 µL) was introduced using the splitless mode. Three different temperature gradients were used for glycolipid analysis, as followed: 90°C (initial); 200°C at 20°C/min (10 min); 230°C at 10°C/min (10 min) and 265°C/min (final 5 min). Spectra which generated at 50-650 *m/z* range at 20 scans per second with the solvent delay of 5 min were collected.

Multivariate Data Analysis

All raw spectrometric data were processed using open-source software MZmine (version 2.2.3). Chromatogram builder, peak detection, spectrum deconvolution, isotope filtering and peak grouping were used for data processing. The detected peaks were subjected to compound identification by searching NIST MS Search 2.0, METLIN database (http://metlin.scripps.edu/), MassBank (http://www.massbank.jp/), LipidMaps (http://www.lipidmaps.org/) and KEGG database (http://www.genome.jp/kegg) using exact molecular weights or MS fragmentation pattern data. The data were further normalised using the total summed metabolites' intensities and transformed by taking the natural log of the intensities' values of the analysed metabolites to make each feature comparable in magnitude to each other. Unsupervised principal component analysis (PCA) was used to analyse the pattern depicting metabolite differences and general clustering. While significantly altered metabolites between groups were identified using supervised partial least squares discriminant analysis (PLS-DA) generated. The values of R^2 and Q^2 parameters were used to verify the fitness and predictive ability of the model. VIP analysis with VIP-score >1.5 was used to determine specific metabolites backing most significantly to the differences recognised by PLS-DA. Significantly different metabolites were then used to generate correlation heatmap identifying metabolites that cluster according to sample groups (healthy or infected). Distance measure was generated by Pearson correlations and clustering using the Ward algorithm.

Identification of Altered Metabolic Pathways

To identify the most relevant metabolic pathways involved in *G. boninense*-oil palm interaction, metabolic pathway analysis and pathway topology analysis were performed using MetPA, a web-based metabolomics tool for pathway analysis and visualisation (http://metpa.metabolomics.ca/MetPA) according to method described by Chen *et al*. (2015). The functional pathway analysis of potential biomarkers was based on the database source of the

Kyoto Encyclopedia of Genes and Genomes (KEGG) (http://www.genome.jp/kegg/). The pathway topology analysis performed was as described by Fan *et al*. (2018) where the impact-value threshold was set as 0.10 and calculated from the analysis, any value above the threshold were rejected as potentially significant pathways.

Potential Biomarkers Identification

Potential biomarkers identification using Receiver Operating Characteristic (ROC) curve analysis was adopted from Barros *et al*. (2018) with some adjustments, by focusing on biomarkers that significantly altered in their metabolite's pathway. ROC analysis of the ROC curve analysis was conducted using the online ROCCET (http://www.roccet.ca). The area under the ROC curve (AUC) was used to calculate the sensitivity and specificity trade-offs. Areas under the ROC curve (AUC) is the method of choice for evaluating the performance of potential biomarkers: the greater the AUC (>0.7), the better the prediction of the model. Potential biomarkers with high sensitivity when infected with *Ganoderma* and low sensitivity when disease is absent were selected.

RESULTS AND DISCUSSION

Assessment of Infection

In the present work, successful inoculation was achieved using RWB technique as similar symptoms were developed at lower stem and bole tissues of inoculated oil palm seedlings, besides the presence of small white button (*Figure 1*) as described by Alizadeh *et al.* (2011); Naher *et al.* (2011); Nur Ain Izzati and Abdullah (2008). All *Ganoderma*-inoculated seedlings showed symptoms of infection after three (first interval) and six months (second interval) post-AI. To further confirm the success of colonisation of the pathogen in roots, *G. boninense* was isolated from the infected oil palm seedling roots using GSM. Positive result on GSM was also correlated with the detection of ergosterol content extracted from roots of inoculated seedlings according to the method demonstrated by Chong *et al*. (2012a). Ergosterol is a sterol component largely restricted to fungi and is absent in another living biomass. No ergosterol was detected in healthy seedlings. Symptoms of *Ganoderma* infection and signs of the presence of *Ganoderma* on inoculated seedlings of the eight months old OP seedlings were noticed as early as three months after inoculation. The uninoculated seedlings did not show any symptoms of BSR infection and remained healthy until the end of the experiment. At first interval, concentration of ergosterol was 39.17 µg/g, DI = 100% and DSI = 30%, meanwhile at second interval, the concentration of ergosterol increased significantly to 186.74 µg/g, DI = 100% parallel to the increased of DSI = 77.5% (*Table 3*) [data and calculation for ergosterol were obtained according to Chong *et al*. (2012a)]. Although some of the infected palms showed symptoms of BSR, DSI percentage at first interval was only 30% as most of the infected seedlings had lower score, thus, this stage was regarded as early infection due to the non-synchronous nature of BSR development (Rees *et al.*, 2009). At second interval, progression of DSI was also in accordance with bole damage index of 47.5% (*Table 3*). All symptoms appeared at second interval, thus, regarded as 'late infection' stage of BSR disease.

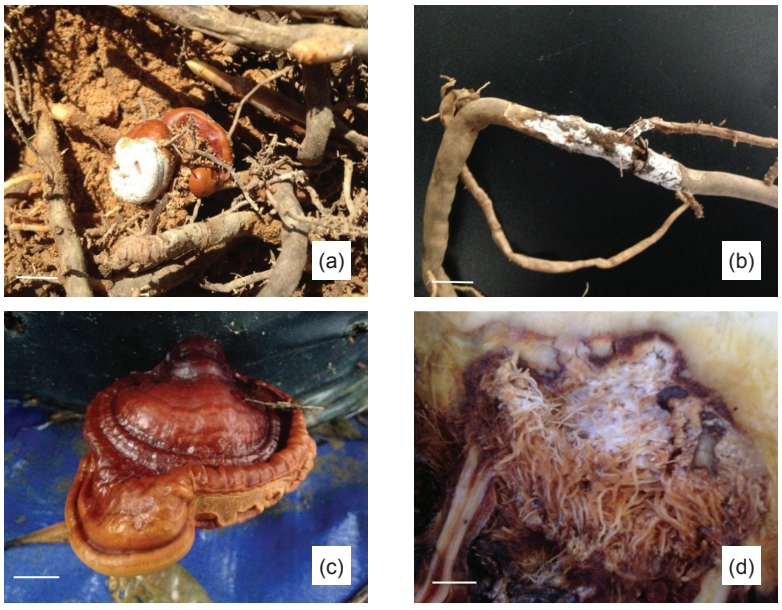

Figure 1. Physical evidence of successful artificial inoculation using Rubber Wood Block technique during first interval (a-b) and second interval (c-d). Bar=1 cm.

TABLE 3. DISEASE ASSESSMENT OF TWO-TIME INTERVALS OF OIL PALM SEEDLINGS INOCULATED WITH *Ganoderma*

Item	First interval	Second interval
Disease incidence (DI)	100%	100%
Ergosterol (μg/g)	39.17 ± 0.75*	186.74 ± 0.84*
Disease severity index (DSI; %)	30*	77.5*
Bole damage index (%)	0*	47.5*

Note: *Significantly different at $p \leq 0.05$ by Tukey comparison test in their respective assessment. Values are the means of 10 replicates, where each replicate consists of a seedling.

Differential Expression and Profile of Glycolipids Composition Related to *Ganoderma* Infection

The differential metabolites between different sample groups were categorised according to the stage of infection assessed at two different intervals. Univariate statistical analysis performed on H-T1 (Healthy-First Interval) and IN-T1 (Infected-First Interval) datasets identified 31 glycolipids were significantly affected at first interval ($\log_2$ (FC) > 2 and p-value < 0.05). Evaluation by PCA showed a clearly different distribution along PC1 covering 86.5% of the total variance (data not shown). In PLS-DA analysis, the components also showed the separation pattern similar to PCA analysis (*Figure 2a*). Using a VIP score of larger than 1.2 as a cut-off, six metabolites were found highly important to the separation (*Figure 2*). In IN-T1 dataset, pyruvic acid was down-regulated, while phosphatidic acid (PA) [18:4(6Z,9Z,12Z,15Z)/0:0], PA (14:0/0:0), phosphatidylcholine (PC) (2:0/2:0), PA (16:0/0:0) and γ-linoleic acid shows up-regulation trend in relative to H-T1. The glycolipids produced by various microorganisms contain different mono- or disaccharides, conjugated with long-chain fatty acids or hydroxyl fatty acids through either acetyl or glycosidic linkages, and some of them exhibit antibiotic (Teichmann *et al*., 2011). The preferential loss of a fatty acid molecule from the glycerol backbone is most likely due to kinetic control of the gas-phase fragmentation process, thus, leading to detection of fatty acids in glycolipids analysis (Zianni *et al*., 2013).

At second interval, 48 metabolites were significantly regulated upon *G. boninense* infection. PCA model for the classification of the H-T2 (Healthy-Second Interval) and IN-T2 (Infected-Second Interval) groups obtained satisfactory validation with 85.1% variance along PC1 (data not shown). The PLS-DA model was used to elucidate the most reliable class-discriminating metabolites that were highly diagnostic for group separation (*Figure 2b*). Together with the VIP scores (>1.2) from the PLS-DA model, five metabolites with highest values were identified, out of which, two metabolites (pyruvic acid and lignoceric acid) were down-regulated, while valeric acid, myriocin and (4E,6E,d14:2) sphingosine were found up-regulated in IN-T2 groups (*Figure 2b*). Glycolipids profiling in the infected samples changed most significantly from their healthy controls at second interval, compared to first interval suggesting regulation of primary metabolism also occurs during plant-pathogen interactions. Using univariate analysis, IN-T1 *vs.* H-T1 and IN-T2 *vs.* H-T2 shared one metabolite, pyruvic acid that was down-regulated in infected samples at both intervals. Evidence for the role of glycolipids in plant defense responses has been provided by experiments showing the induction of genes involved in carbohydrate metabolism upon challenge by pathogens or pathogen-derived elicitors (Rojas *et al*., 2014).

Apparently, fatty acid consisting of odd number of carbon atom chain, such as valeric acid might contribute to the regulation of systemic induced resistance (Kuć and Tuzun, 1990). Detection of myriocin, fungal secondary metabolites is one of most widely studied extraordinary sphingoid bases. Intriguingly, in spite of increased accumulation of myriocin, a long-chain sphingoid base, (4E,6E,d14:2) sphingosine was also increased simultaneously. These long-chain bases are important intermediates and signalling molecules in the sphingolipid catabolic pathway (Speigel and Milstien, 2002). The levels of long-chain bases in healthy tissues are usually low, however study found treatment of corn tissue with mycotoxins can increase their level dramatically (Wright *et al*., 2003). Plant-pathogen interactions have implicated disruption of sphingolipid synthesis and build-up of long-chain bases during the hypersensitive response in programmed cell death associated with the plant defense response. The toxins myriocin resulting in an accumulation of sphingiocine associated with plant necrosis promotion (Tanaka *et al*., 1993) and programmed cell death (apoptosis) in plant tissues (Wang *et al*., 1996), is related to their detection in second interval. The response to these toxins may be complex and apparently involves the participation of several signalling pathways (Asai *et al*., 2000), which lead to long-chain bases accumulation and cell death. But if long-chain base synthesis is concurrently inhibited, long-chain base build-up is prevented and the toxic effects are at least partly blocked (Spassieva *et al*., 2002). These findings propose that sphingoid long-chain bases may be significant in signalling or regulatory roles in plant defense, and higher levels in plant tissues lead to cell death.

To identify the changes in glycolipid composition between infected and healthy samples at first and second interval, multivariate statistical analysis was performed. To answer a question which the first two t-tests was unable to address, an analysis of variance (ANOVA) test was conducted

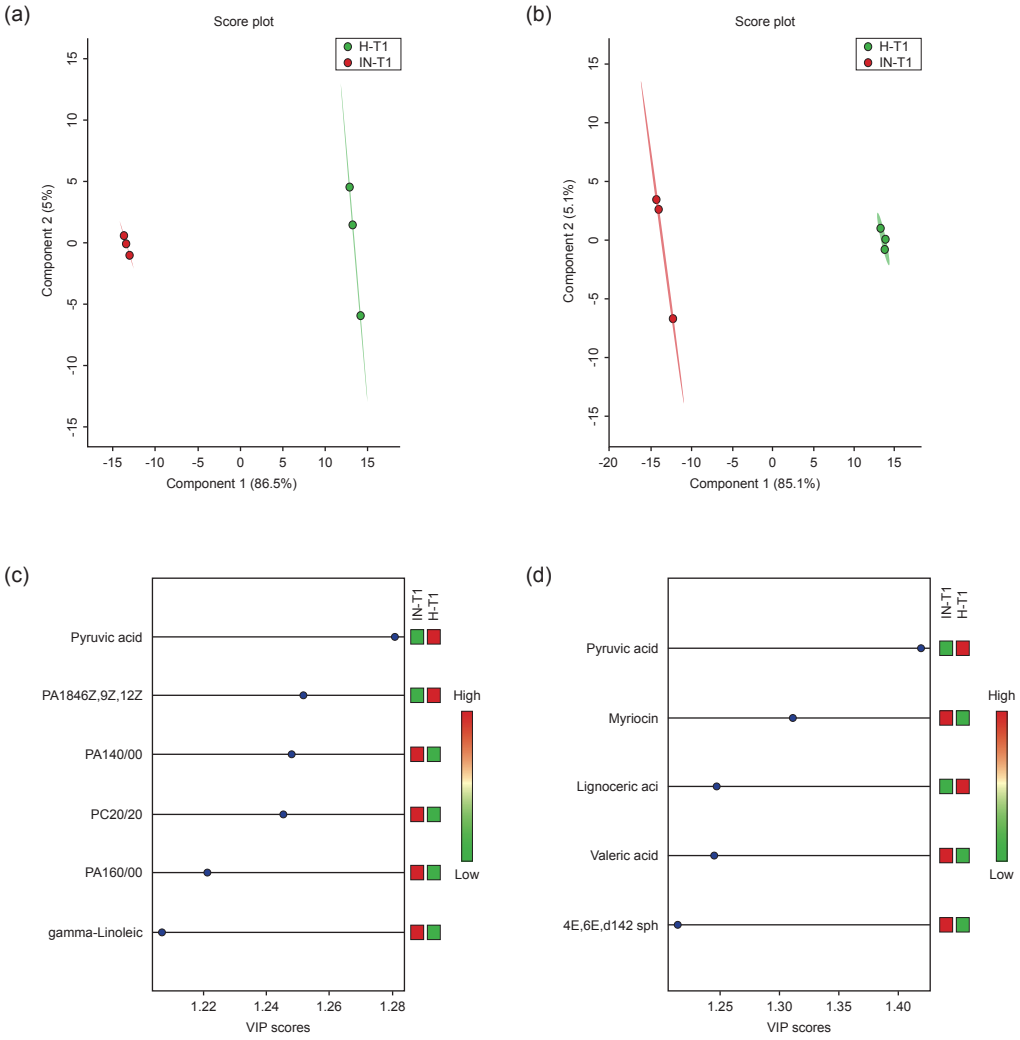

Note: H=Healthy seedlings; IN=*Ganoderma*-inoculated seedlings; T1=First interval (three months post-artificial inoculation (AI)); T2=Second interval (six months post-AI).

Figure 2. Partial least square-discriminant analysis (PLS-DA) of (a) IN-T1 vs. *H-T1 and (b) IN-T2* vs. *H-T2; variable importance in projection (VIP) score plot selected from PLS-DA model with p>0.05 and (VIP) scores >1.2 of (c) IN-T1* vs. *H-T1 and (d) IN-T2* vs. *H-T2. Colour key indicates metabolite expression value, green: Lowest, red: highest. Analysis by Metaboanalyst consists n=3 replicates for each group.*

to identify the common changes in glycolipids profiles. ANOVA test revealed a total of 31 significant features with *p*-value <0.05. PCA showed that 79.5% of the total variance in the data was represented by the first two principal components (*Figure 3a*). PCA scores plot show H-T1, H-T2 and IN-T1 were separated from IN-T2 along PC1, indicating that IN-T1 and IN-T2 profiles were very distinct to each other. To obtain a more reliable statistical analysis and specific loadings, a PLS-DA model was used to discriminate healthy and infected groups. PLS-DA was able to discriminate lipid samples based on the treatment they received with good cross-validated model performance using the first two latent variables (R^2 = 0.972; Q^2 = 0.945). PLS-DA additionally informed upon which metabolites were most important for the classification model via their VIP scores and identified nine metabolites (VIP values >1.5) (*Figure 3b*). Further analysis using heatmap recognised two metabolites (Pyruvic acid and lignoceric acid), from healthy (H-T1 and H-T2) groups showing highly significant of differences from infected groups, suggesting that these two metabolites might significantly perturbed during *G. boninense* infection (*Figure 3c*). Pyruvic acid, a product of glycolysis and very-long-chain fatty acids such as lignoceric acid exert crucial functions in plant developmental processes, thus, when their levels are perturbed marked phenotypic consequences in plant growth (De Bigault Du Granrut and Cacas, 2016). Meanwhile, ethyl heptanoate, PC (6:0/0:0), PC (2:0/2:0), γ-linoleic acid, methyl stearate, PA [18:4(6Z,9Z,12Z,15Z)/0:0] and PA (14:0/0:0) were significantly up-regulated in

IN-T1 and IN-T2 samples. These metabolites could be used as potential biomarkers to discriminate infected and healthy oil palm seedlings. Production of biologically active lipids, such as PA and PC has been identified as a major source of lipid second messenger and play an important role in signal transduction. Increases in PA concentration have been observed under various environmental stresses and detected during early response in the *Cladosporium fulvum*-4/Avirulence-4 interaction (de Jong *et al*., 2004). Induction of reactive oxygen species (ROS) formation is also linked to PA (Park *et al*., 2004). Signal-induced production of PA in the cell is accompanied by increases of PC, in contrast with other study by Xie *et al.* (2015). Accumulation of PC might derive from the pathogen's membrane cell (Siebers *et al*., 2016). Increased level of methyl stearate was also in parallel with the findings in vegetative tissues of sunflower mutants (Cantisán *et al*., 1999). This compound is converted into linoleic acid, a precursor for the defense signalling molecules jasmonic acid (Wang *et al*., 2017). Jasmonic acid functions as a trigger to the phenylpropanoid pathway to increase the synthesis of phenolic compounds (Gundlach *et al*., 1992). Significant increment of γ-linoleic acid was also consistently observed in *Arabidopsis thaliana* infected with *Sclerotinia sclerotiorum* at all-time point (3, 6 and 24 hr after infection). Linoleic acid was also associated in pathogenesis and resistance-related metabolites of wheat, upon infection with *Fusarium* head blight disease (Hamzehzarghani *et al*., 2008). No previous evidence on accumulation of ethyl heptanoate has been reported elsewhere.

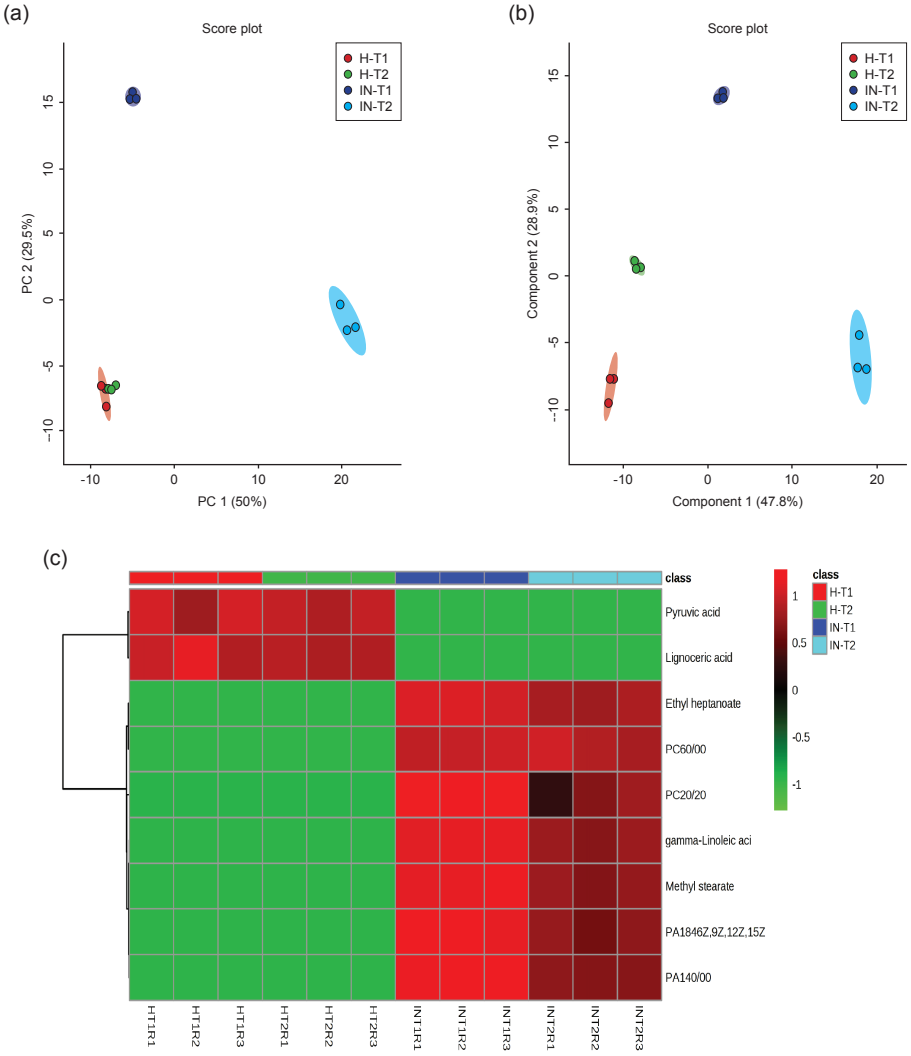

Note: H=Healthy seedlings; IN=*Ganoderma*-inoculated seedlings; T1=First interval [three months post-artificial inoculation (AI)]; T2=Second interval (six months post-AI).

Figure 3. Multivariate cluster analysis of glycolipids profiles of H-T1 vs. *IN-T1* vs. *H-T2* vs. *IN-T2 at first and second intervals. (a) Score-plot of principal component analysis (PCA), (b) Score-plot of partial least square-discriminant analysis (PLS-DA), and (c) Heatmap visualisation analysis of metabolites (VIP score >1.5; p>0.05) identified from PLS-DA model with a potential identity to distinguish between infected and healthy groups. Colour key indicates metabolite expression value, green: Lowest, red: highest. Analysis by Metaboanalyst consists n=3 replicates for each group.*

Metabolite Pathways Related to *G. boninense* Infection

Metabolic pathway analysis was performed to reveal the most relevant pathways related to *Ganoderma* infection. The impact score (IS) of these pathways calculated from pathway topology analysis above 0.10 was screened out as potential target pathway. Significant features with *p*-value<0.05 and PLS-DA VIP score >1.5 from multivariate analyses were pooled and further subjected to pathway analysis. The result in *Figure 4* shows that two pathways; pyruvate metabolism (IS: 0.1129) and glycolysis or gluconeogenesis (IS: 0.1091) were associated with *G. boninense* throughout the whole experiment. As a hemibiotrophic fungal pathogen, *G. boninense* first establishes a biotrophic interaction with the host plant and later switches to a destructive necrotrophic lifestyle. This study suggested that when the fungus breaches into host CW to access nutrients that are available in the starch reservoir (biotroph stage) (Rees *et al.*, 2009), causes the host plant to induce the signaling pathway and defensive environment. Fascinatingly however, *G. boninense* seems to be able to avoid direct contact with the defense compounds produced by the defensive signalling pathway, causing the infection progresses to the latent and later stage of BSR disease as demonstrated in Glucosinolate metabolites for *Arabidopsis thaliana* defense mechanism against several pathogens (Clay *et al.*, 2009). When *G. boninense* initiates the necrotrophic program, it causes interference with the carbohydrate metabolism pathways (Su *et al.*, 2021). *Ganoderma boninense* invasion substantially alters the primary metabolism of oil palm roots seedlings as seen by the downregulation of pyruvic acid and carbohydrate metabolism at first and second intervals. Pyruvic acid declines early in the infection process and continues to decline during the biotrophic stage. In this study, it was suggested that *G. boninense* avoided effective defenses by hijacking pyruvic acid-associated pathways as shown in *Figure 4*. During *G. boninense* colonisation, OP seedling induced the downregulation of pyruvic acid, involved in carbohydrate catabolism processes such as glycolysis or gluconeogenesis and pyruvate metabolism. It has been suggested that the energy saved by down-regulation of primary metabolism is diverted and used for defense responses (Rojas *et al.*, 2014). As plant defense responses require abundant supply of energy, primarily derived from primary metabolic processes (Bolton, 2009). However, the ability of *G. boninense* to utilise plant-carbohydrate upon colonisation decreases this metabolite thus, weaken the oil palm into 'starvation', consequently exposed to *G. boninense* colonisation (Divon and Fluhr, 2007; Li *et al.*, 2019).

Identification of Biomarkers Associated with *G. boninense* Infection

Biomarkers were identified using a subset of metabolites from the multivariate statistical analyses outlined earlier, as these metabolites were capable of discriminating between sample groups. ROC analysis was performed to further characterise the predictive value of selected metabolites independently. Disease analysis employs the ROC

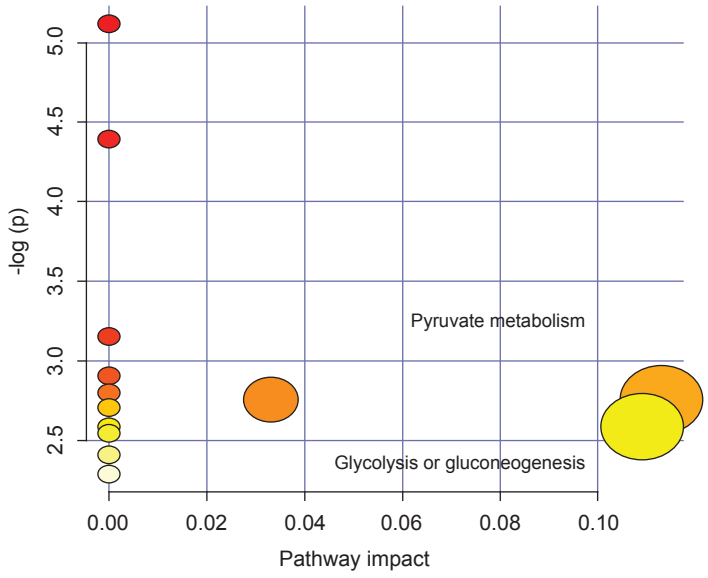

Figure 4. The pathway impact analysis of cell-wall lipid metabolites selected from multivariate analysis (from whole experiment) using MetPA. Each circle represents a matched pathway. Metabolic pathways with impact values >0.05 were considered to be perturbed.

curve and the area under the ROC curve (AUC) to obtain a numerical value of the relationship between the specificity and sensitivity of a biomarker. The sensitivity and specificity indicate the probability tests for correctly identifying infected palms with the disease and without the disease, respectively (Lalkhen and McCluskey, 2008). AUC value of 1.0 shows a perfect prediction in term of the sensitivity and specificity of the diagnostic test (Greiner *et al.*, 2000), thus, these metabolites could be used as biomarkers to differentiate the infected and healthy tissues. To confirm the prediction of *Ganoderma*-infected tissue, a combination of more than one discriminatory metabolite was developed via logistic regression analysis and showed that the combination of metabolite also resulted to a better discriminator with AUC equal to 1 (*Figure 5a*), and a clear separation and discrimination were observed between the infected and healthy samples in the probability view (*Figure 5b*). The average accuracy based on 100 cross validations (CV) was 1 in this study (*Figure 5c*). Having an average accuracy close to 1 indicates a more valid CV prediction. Box-whisker plots revealed that all five biomarkers exhibited significantly higher levels in infected samples than in healthy ($p<0.05$) (*Figure 6*). Since the five biomarkers showed the AUC value of 1.0, they were selected as biomarkers of infected palms.

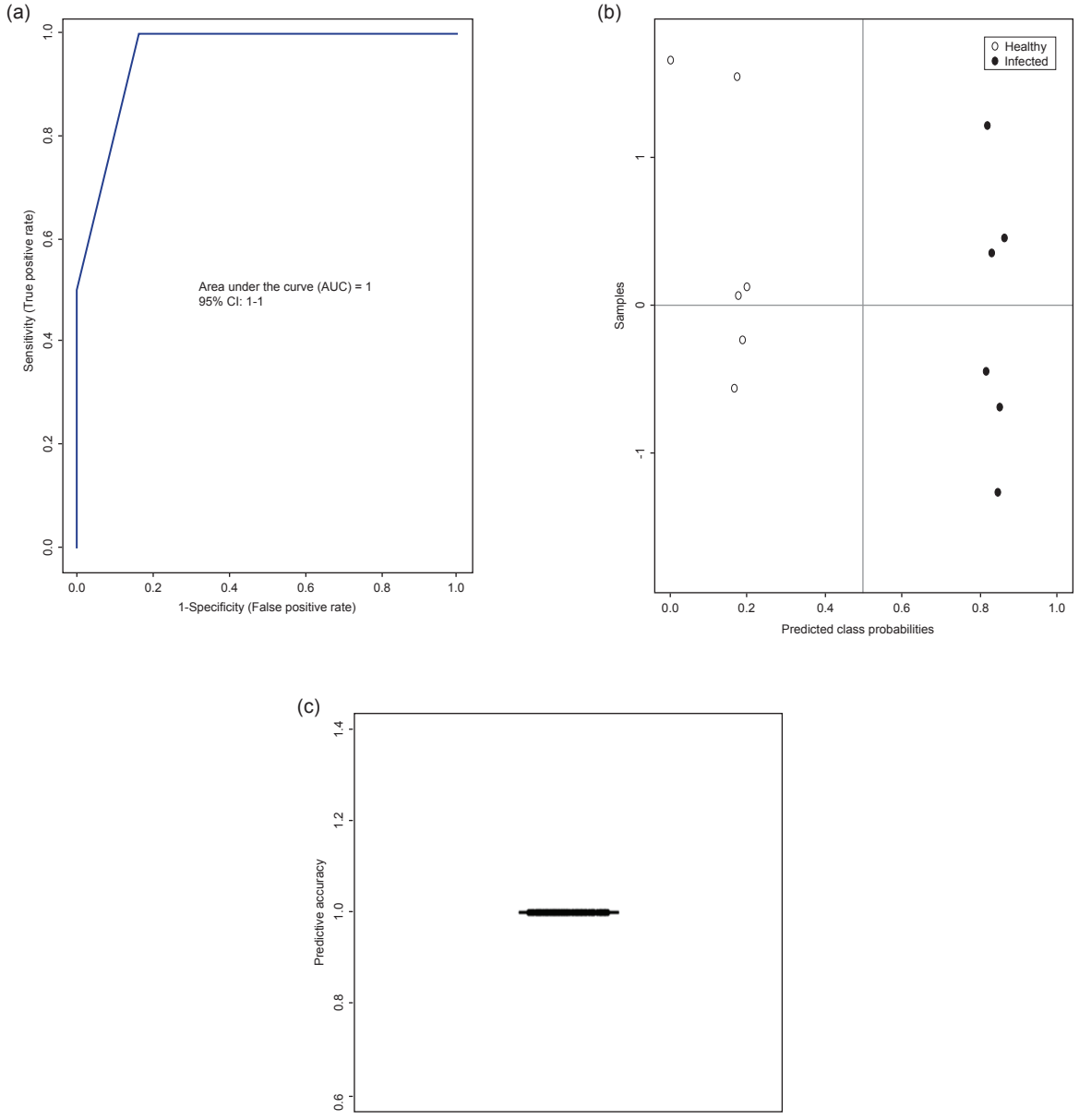

Figure 5. Biomarker analysis results (ROC view). Statistical method to evaluate infected and healthy discrimination using selected potential metabolites. (a) Probability view, (b) cross validation prediction, and (c) accuracy of selected metabolites, PC (6:0/0:0), PC(2:0/2:0), PA(18:4(6Z,9Z,12Z,15Z)/0:0), PA(14:0/0:0) and γ-linolenic acid.

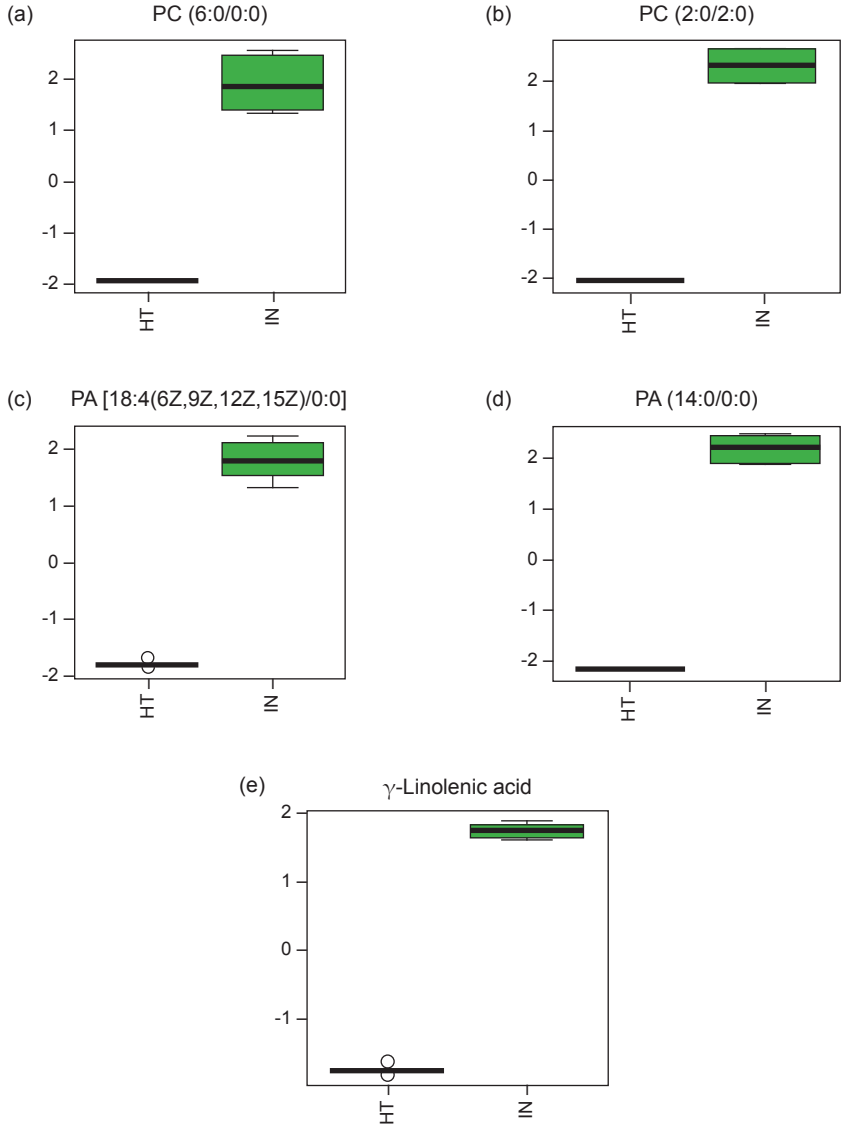

Figure 6. Box-and-whiskers plots representing relative abundance of (a) PC(6:0/0:0); (b) PC(2:0/2:0); (c) PA(18:4(6Z,9Z,12Z,15Z)/0:0); (d) PA(14:0/0:0); (e) γ-linolenic acid in Ganoderma-*infected and healthy oil palm seedlings. The relative abundance of each metabolite in lipid profiles of* Ganoderma-*infected was significantly higher than healthy groups using Student's t-test (p-value <0.05).*

CONCLUSION

The current study indicates lipid-profiling techniques combined with chemometric analysis can develop a detailed picture and provide a broader assessment of the glycolipid change that occur in oil palm roots CW in response to the BSR disease. The study provides an insight into complex host-pathogen interactions, and also discovers altered lipidomics/metabolomics pathways involved in disease pathogenesis. Pyruvate metabolism and glycolysis or gluconeogenesis are the most perturbed pathways during the pathogenesis. Simulation of defense pathway using synthesised metabolites in oil palm may probably lead to the enhancement of defense reactions, leading to the formation of physiochemical reactions barrier which preventing the invasion of *G. boninense*. The five metabolites: PC(6:0/0:0), PC(2:0/2:0), PA[18:4(6Z,(Z,12Z,15Z)/0:0], PA(14:0/0:0) and γ-linolenic acid which had been identified and analysed in the present work could be used as diagnostic biomarkers to identify *G. boninense* infection and allow an earlier control. Future research using genetic approach on these biomarkers will deepen the understanding of their importance in defense/cell signaling and the role of glycolipid in plant-pathogen interaction in essence to hastening the development of BSR early detection approach.

ACKNOWLEDGEMENT

The authors wish to thank Ministry of Higher Education of Malaysia for funding the project through the Fundamental Research Grant Scheme (FRG0342-ST-2/2013). Support and service provided by the Universiti Malaysia Sabah are also gratefully acknowledged.

REFERENCES

Abdulllah, F; Ilias, G N M; Nelson, M; Nur Ain Izzati, M Z and Umi Kalsom, Y (2003). Disease assessment and the efficacy of *Trichoderma* as a biocontrol agent of basal stem rot of oil palm. *Res. Bull. Sci. Putra*, *11*: 31-33.

Alexander, A; Abdullah, S; Rosall, S and Chong, K P (2017). Evaluation of the efficacy and mode of action of biological control for suppression of *Ganoderma boninense* in oil palm. *Pak. J. Bot.*, *49(3)*: 1193-1199.

Alizadeh, F; Abdullah, S N A; Khodavandi, A; Abdullah, F; Yusuf, U K and Chong, P P (2011). Differential expression of oil palm pathology genes during interactions with *Ganoderma boninense* and *Trichoderma harzianum*. *J. Plant Physiol.*, *168*: 1106-1113.

Ariffin, D and Idris, A S (1992). The *Ganoderma* selective medium (GSM). *PORIM Information Series No. 8*.

Ariffin, D; Idris, A S and Singh, G (2000). Status of *Ganoderma* in oil palm. *Ganoderma Diseases of Perennial Crops* (Flood, J; Bridge, P D and Holderness, M eds.). CABI Publishing, Wallingford. p. 49-68.

Asai, T; Stone, J M; Heard, J E; Kovtun, Y; Yorgrey, P; Sheen, J and Ausubel, F M (2000). Fumonisin B1-induced cell death in *Arabidopsis* protoplasts requires jasmonate-, ethylene-, and salicylate-dependent signaling pathways. *Plant Cell, 12*: 1823-1835.

Barros, R P C; da Cunha, E V I; Catão, R M R; Scotti, L; Souza, M S R; Brás, A A Q and Scotti, M T (2018). Virtual screening of secondary metabolites of the genus Solanum with potential antimicrobial activity. *Rev. Bras. Farmacogn.*, *28*: 686-691.

Bolton, M D (2009). Primary metabolism and plant defense - Fuel for the fire. *Mol. Plant Microbe Interact., 22*: 487-497.

Cantisán, S; Martínez-Force, E; Álvarez-Ortega, R and Garcés, R (1999). Lipid characterization in vegetative tissues of high saturated fatty acid sunflower mutants. *J. Agric. Food Chem.*, *47(1)*: 78-82.

Canut, H; Albenne, C and Jamet, E (2016). Isolation of the cell wall. *Isolation of Plant Organelles and Structures. Methods in Molecular Biology.* (Taylor, N and Millar, A eds.). Vol. 1511: Humana Press, New York, USA. p. 171-185.

Chen, H-H; Tseng, Y J; Wang, S-Y; Tsai, Y-S; Chang, C-S; Kuo, T-C; Yao, W-J; Shieh, C-C; Wu, C-H and Kuo, P-H (2015). The metabolome profiling and pathway analysis in metabolic healthy and abnormal obesity. *Int. J. Obes.*, *39(8)*: 1241-1248.

Chong, K P; Atong, M and Rossall, S (2012a). The role of syringic acid in the interaction between oil palm and *Ganoderma boninense*, the causal agent of Basal Stem Rot. *Plant Pat., 61*: 953-963. DOI: 10.1111/j.1365-3059.2011.02577x.

Chong, K P; Atong, M and Rossall, S (2012b). The roles of syringic, caffeic and 4-hydroxybenoic acid in *Ganoderma*-oil palm interaction. *Asian J. Microbiol. Biotechnol. Environ. Sci.*, *14(2)*: 157-166.

Chong, K P; Abdullah, S and Ng, T L (2013). Molecular fingerprint of *Ganoderma* spp. from Sabah, Malaysia. *Int. J. Agric. Biol.*, *15*: 1112-1118.

Chong, K P; Dayou, J and Alexander, A (2017). *Detection and Control of Ganoderma Boninense in Oil Palm Crop*. Springer Briefs in Agriculture. Springer, Cham. 77 pp.

Chong, K P; Eldaa, P A and Dayou, J (2014). Relation of *Ganoderma* ergosterol content to basal stem rot disease severity index. *Adv. Environ. Biol.*, *8(14 (Special))*: 14-19.

Clay, N K; Adio, A M; Denoux, C; Jander, G and Ausubel, F M (2009). Glucosinolate metabolites required for an *Arabidopsis* innate immune response. *Science*, *323(5910)*: 95-101.

Dayou, J; Alexander, A; Sipaut, C S; Chong, K P and Lee, P C (2014). On the possibility of using FTIR for detection of *Ganoderma boninense* in infected oil palm tree. *Int. J. Adv. Agric. Environ. Eng.*, *1(1)*: 161-163.

De Bigault Du Granrut, A and Cacas, J L (2016). How very-long-chain fatty acids could signal stressful conditions in plants? *Front. Plant Sci.*, *7*: 1490.

de Jong, C F; Laxalt, A M; Bargmann, B O; de Wit, P J; Joosten, M H and Munnik, T (2004). Phosphatidic acid accumulation is an early response in the *Cf-4*/*Avr4* interaction. *Plant J.*, *39*: 1-12.

Divon, H H and Fluhr, R (2007). Nutrition acquisition strategies during fungal infection in plants. *FEMS Microbiol. Lett.*, *266 (1)*: 65-74.

Fan, W; Ge, G; Liu, Y; Wang, W; Liu, L and Jia, Y (2018). Proteomics integrated with metabolomics: Analysis of the internal causes of nutrient changes in alfalfa at different growth stages. *BMC Plant Biol.*, *18(1)*: 1-15.

Greiner, M; Pfeiffer, D and Smith, R D (2000). Principles and practical application of the receiver-

operating characteristic analysis for diagnostic tests. *Prev. Vet. Med.*, *45*: 23-41.

Gundlach, H; Müller, M J; Kutchan, T M and Zenk, M H (1992). Jasmonic acid is a signal transducer in elicitor-induced plant cell cultures. *Proc. Natl. Acad. Sci. USA*, *89*: 2389-2393.

Hamzehzarghani, H; Paranidharan, V; Abu-Nada, Y; Kushalappa, A C; Mamer, O and Somers, D (2008). Metabolic profiling to discriminate wheat near isogenic lines, with quantitative trait loci at chromosome 2DL, varying in resistance against *Fusarium* head blight. *Can. J. Plant Sci.*, *88*: 789-797.

Idris, A S; Mazliham, M S and Madihah, A Z (2009). Current technologies for detection of *Ganoderma* in oil palm. *Proc. Agric. Biotechnol. Sustain. Conf.-PIPOC*. MPOB, Bangi. p. 81-98.

Ishaq, I; Alias, M S; Kadir, J and Kawawani, I (2014). Detection of basal stem rot disease at oil palm plantations using sonic tomography. *J. Sustain. Sci. Manag.*, *9(2)*: 52-57.

Japanis, F G; Chan, Y S and Chong, K P (2021). Evaluation on the effectiveness of combination of biocontrol agents in managing *Ganoderma boninense* of oil palm. *Malays. J. Microbiol.*, *17(1)*: 1-10.

Khairudin, H (1991). Pathogenicity of three *Ganoderma* species on oil palm seedlings. *J. Perak Planters Assoc.* p. 43-49.

Kuć, J and Tuzun, S (1990). Metabolic regulation of resistance genes in tobacco for the control of blue mold. *Blue Mold Disease of Tobacco Literature Service* (Main, C and Spurr, H eds.). North Carolina State University, Raleigh. p. 35-46.

Lalkhen, A G and McCluskey, A (2008). Clinical tests: Sensitivity and specificity. *Cont. Edu. Anaesth, Critical Care Pain*, *8*: 221-223.

Lelong, C C; Roger, J-M; Brégand, S; Dubertret, F; Lanore, M; Sitorus, N; Raharjo, D and Caliman, J-P (2010). Evaluation of oil-palm fungal disease infestation with canopy hyperspectral reflectance data. *Sensors (Basel)*, *10(1)*: 734-747.

Li, P; Liu, W; Zhang, Y; Xing, J; Li, J; Feng, J; Su, X and Zhao, J (2019). Fungal canker pathogens trigger carbon starvation by inhibiting metabolism in poplar stems. *Sci. Rep.*, *9*: 10111.

Longo, L V G; Nakayasu, E S; Lopes, F G; Vallejo, M C; Matsuo, A L; Almeida, I C and Puccia, R (2013). Characterization of cell wall lipids from the pathogenic phase of *Paracoccidioides brasiliensis* cultivated in the presence or absence of human plasma. *PLoS ONE*, *8(5)*: e63372.

Madihah, A Z; Maizatul-Suriza, M; Idris, A S; Bakar, M F A; Kamaruddin, S; Bharudin, I; Abu Bakar, F D and Murad, A M A (2018). Comparison of DNA extraction and detection of *Ganoderma,* causal of basal stem rot disease in oil palm using loop-mediated isothermal amplification. *Malays. Appl. Biol. J.*, *47(5)*: 119-127.

Markon, M A; Shakaff, A Y; Adom, A H; Ahmad, M N and Abdullah, A H (2008). The feasibility study of utilising electronic nose and ANN for plant malaise detection. *Proc. MUCET Malaysian Universities Conf. Eng. Technol. (MUCET)*. Putra Brasmana, Perlis, Malaysia. p. 1-6.

Masood, A; Saeed, S; Iqbal, N; Malik, M T and Kazmi, M R (2010). Methodology for the evaluation of symptoms severity of mango sudden death syndrome in Pakistan. *Pak. J. Bot.*, *42(2)*: 1289-1299.

Michael, M L; Chong, K P; Zenian, S; Lo, A S V and Dayou, J (2020). On the propagation of *Ganoderma boninense* infection of basal stem rot in oil palm with the aid of acoustics computed assisted tomography. *Tran. Sci. Tech., 7(3-2)*: 165-171.

Mille-Lindblom, C; von Wachenfeldt, E and Tranvik, L J (2004). Ergosterol as a measure of living biomass: Persistance in environmental samples after fungal death. *J. Microbiol. Methods*, *59*: 253-262.

Mohd As'wad, A W; Sariah, M; Paterson, R R M; Zainal Abidin, M A and Lima, N (2011). Ergosterol analyses of oil palm seedlings and plants infected with *Ganoderma*. *Crop Prot.*, *30*: 1438-1442.

Naher, L; Ho, C-L; Tan, S G; Yusuf, U K and Abdullah, F (2011). Cloning of transcripts encoding chitinases from *Elaeis guineensis* Jacq. and their expression profiles in response to fungal infections. *Physiol. Mol. Plant Pathol.*, *76*: 96-103.

Najmie, M M K; Khalid, K; Sidek, A A and Jusoh, M A (2011). Density and ultrasonic characterization of oil palm trunk infected by *Ganoderma boninense* disease. *Meas. Sci. Rev.*, *11(5)*: 160-164.

Nur Ain Izzati, M Z and Abdullah, F (2008). Disease suppression in *Ganoderma*-infected oil palm seedlings treated with *Trichoderma harzianum*. *Plant Protect. Sci.*, *44*: 101-107.

Nursabrina, A A; Sariah, M and Zaharah, A R (2012). Suppression of basal stem rot disease progress on oil palm (*Elaeis guineensis*) after copper and calcium

supplementation. *Pertanika J. Trop. Agric. Sci.*, *35*: 13-24.

Nyberg, H (1986). GC-MS methods for lower plant glycolipid fatty acids. *Gas Chromatography/Mass Spectrometry* (Linskens, H F and Jackson, J F eds.). Modern Methods of Plant Analysis (New Series). Vol. 3. Springer, Berlin, Heidelberg. p. 67-99.

Park, J; Gu, Y; Lee, Y; Yang, Z and Lee, Y (2004). Phosphatidic acid induces leaf cell death in *Arabidopsis* by activating the Rho-related small G protein GTPase- mediated pathway of reactive oxygen species generation. *Plant Physiol.*, *134*: 129-136.

Rees, R W; Flood, J; Hasan, Y; Potter, U and Cooper, R M (2009). Basal stem rot of oil palm (*Elaeis guineensis*); mode of root infection and lower stem invasion by *Ganoderma boninense*. *Plant Pathol.*, *58*: 982-989.

Rojas, C M; Senthil-Kumar, M; Tzin, V and Mysore, K S (2014). Regulation of primary plant metabolism during plant-pathogen interactions and its contribution to plant defense. *Front. Plant Sci.*, *5(17)*: 1-11.

Siebers, M; Brands, M; Wewer, V; Duan, Y; Georg, H and Peter, P (2016). Lipids in plant-microbe interactions. *Biochim. Biophys. Acta Mol. Cell Biol. Lipids*, *1861(9)*: 1379-1395.

Spassieva, S D; Markham, J E and Hille, J (2002). The plant disease resistance gene *Asc-1* prevents disruption of sphingolipid metabolism during AAL-toxin induced programmed cell death. *Plant J.*, *32*: 561-572.

Spiegel, S and Milstien, S (2002). Sphingosine 1-phosphate, a key cell signaling molecule. *J. Biol. Chem.*, *277*: 25851-25854.

Stobiecki, M; Wojtaszek, P and Gulewicz, K (1997). Application of solid phase extraction for profiling quinolizidine alkaloids and phenolic compounds in *Lupinus albus*. *Phytochem. Anal.*, *8(4)*: 153-158.

Su, T; Zhou, B; Cao, D; Pan, Y; Hu, M; Zhang, M; Wei, H and Han, M (2021). Transcriptomic profiling of *Populus* roots challenged with *Fusarium* reveals differential responsive patterns of invertase and invertase inhibitor-like families within carbohydrate metabolism. *J. Fungi*, *7(2)*: 89.

Tanaka, T; Abbas, H K and Duke, S O (1993). Structure-dependent phytotoxicity of fumonisins and related compounds in duckweed bioassay. *Phytochemistry*, *33*: 779-785.

Tay, Z H and Chong, K P (2016). The potential of papaya leaf extract in controlling *Ganoderma boninense*. *IOP Conf. Series: Earth and Env. Sci., 36(1)*: 012027.

Teichmann, B; Lefebvre, F; Labbé, C; Bölker, M; Linne, U and Bélange, R R (2011). Beta hydroxylation of glycolipids from *Ustilago maydis* and *Pseudozyma flocculosa* by an NADPH-dependent β-hydroxylase. *Appl. Environ. Microbiol.*, *77*: 7823-7829.

Toh Choon, R L; Sariah, M and Siti Mariam, M N (2012). Ergosterol from the soilborne fungus *Ganoderma boninense*. *J. Basic Microbiol.*, *52*: 608-612.

Wang, H; Li, J; Bostock, R M and Gilchrist, D G (1996). Apoptosis: A functional paradigm for programmed plant cell death induced by a host selective phytotoxin and invoked during development. *Plant Cell*, *8*: 375-391.

Wang, X; Li, J and Zhu, P (2017). Effect of *Sclerotinia sclerotiorum* on lipid metabolism in *Arabidopsis thaliana*. *J. Plant Dis. Prot.*, *124(5)*: 421-426.

Wright, B S; Snow, J W; O'Brien, T C and Lynch, D V (2003). Synthesis of 4-hydroxysphinganine and characterization of sphinganine hydroxylase activity in corn. *Arch. Biochem. Biophys.*, *415*: 184-192.

Xie, L-J; Chen, Q-F; Chen, M-X; Yu, L-J; Huang, L; Chen, L; Wang, F-Z; Xia, F-N; Zhu, T-R; Wu, J-X; Yin, J; Liao, B; Shi, J; Zhang, J-H; Aharoni, A; Yao, N; Shu, W and Xiao, S (2015). Unsaturation of very-long-chain ceramides protects plant from hypoxia-induced damages by modulating ethylene signaling in *Arabidopsis*. *PLoS Genetic, 11(3)*: e1005143.

Zianni, R; Bianco, G; Lelario, F; Losito, I; Palmisano, F and Cataldi, T R (2013). Fatty acid neutral losses observed in tandem mass spectrometry with collision-induced dissociation allows regiochemical assignment of sulfoquinovosyl-diacylglycerols. *J. Mass Spectrom.*, *48(2)*: 205-215.